

INNOVATIVE DESIGN AND PERFORMANCE TEST OF THRESHING-SEPARATING DEVICE FOR HORIZONTAL AXIAL-FLOW COMBINE HARVESTER

横轴流联合收获机脱分选装置创新设计与性能试验

Xuan ZHOU^{1,2)}, Zhiming WANG^{1,2*)}, Liquan TIAN^{1,2)}, Zhan SU^{1,2)}, Zhao DING^{1,2)}

¹⁾ Department of Mechanical and Electrical Engineering, Jinhua Polytechnic, Jinhua 321017, China

²⁾ Key Laboratory of Crop Harvesting Equipment Technology of Zhejiang Province, Jinhua 321017, China

E-mail: jhcwzm@163.com

DOI: <https://doi.org/10.35633/inmateh-67-49>

Keywords: combine harvester; differential threshing; threshing-separating system; performance test; regression mathematical model

ABSTRACT

Aiming at the problems of high grain entrainment loss rate and impurity rate of traditional horizontal axial-flow combine harvesters, a horizontal axial-flow threshing-separating device with coaxial differential threshing drum, conical cleaning fan, double-layer vibrating screen and spiral plate-tooth re-thresher is designed. Meanwhile, a test-bed with a feeding rate of 2 kg/s is designed to improve the device performance. The test through quadratic orthogonal rotation combination design method is used to inspect the effects of the differential drum speed combination, conical fan blade taper, and length ratio of the high and low speed sections of the differential drum on the loss rate, crushing rate, impurity rate and threshing power consumption. The regression mathematical models of the loss rate, crushing rate, impurity content and threshing power consumption are established, and the multi-objective optimization calculation of the regression mathematical model is carried out by using MATLAB optimization toolbox. The results show that the order of the three factors affecting the loss rate and impurity content of the horizontal axial-flow threshing-separating device is the differential drum speed combination, the conical fan blade taper, and the length ratio of high and low speed sections of the differential drum. The field test results show that the performance index of the horizontal axial-flow separation device is better than the requirements of the national standard.

摘要

针对传统横轴流联合收获机籽粒夹带损失率和籽粒含杂率高的问题，设计了以同轴差速脱粒滚筒、圆锥形清选风机、双层振动筛和螺旋板齿式复脱器为主要工作部件的横轴流脱分选装置。为了提升横轴流脱分选装置工作性能，设计了喂入量为2 kg/s的试验台，采用二次正交旋转组合设计法进行工作性能试验，考察差速滚筒转速组合、圆锥形风机叶片锥度、差速滚筒高低速段长度配比3个因素对损失率、破碎率、含杂率和脱粒功耗4个性能指标的影响。建立了损失率、破碎率、含杂率、脱粒功耗的回归数学模型，利用Matlab优化工具箱对回归数学模型进行了多目标优化计算。结果表明：影响横轴流脱分选装置损失率、含杂率的3个因素主次顺序依次为差速滚筒转速组合、圆锥形风机叶片锥度、差速滚筒高低速段长度配比；影响横轴流脱分选装置破碎率、脱粒功耗的3个因素主次顺序依次为差速滚筒转速组合、差速滚筒高低速段长度配比、圆锥形风机叶片锥度；最优参数组合为：差速滚筒转速组合750/950 r/min，风机叶片锥度3.8°，高速段比例30%；对应工作性能指标为：损失率1.57%、破碎率0.71%、含杂率0.38%，脱粒功耗6.67 kW/kg。田间试验结果表明，横轴流脱分选装置工作性能指标优于国家标准规定要求。

INTRODUCTION

In the south, in order to adapt to the small field operation, the rod tooth transverse axial-flow single drum combine harvester is widely used for rice harvesting. The quality of threshing, separating and cleaning directly affects the performance of the whole machine. Scholars have carried out simulation and experimental researches on the threshing, separating and cleaning of the combine harvester to improve the performance.

Zhou Xuan, Associate Professor; Wang Zhiming, Professor; Tian Liquan, Associate Professor; Su Zhan, Lecturer; Ding Zhao, Associate Professor.

In threshing, scholars have done a lot of research on the movement process and stress of materials in the threshing device under different grain varieties' water content, maturity, harvest time and different feeding rates (Li et al., 2014; Miu and Kutzbach, 2007; Miu and Kutzbach, 2008). The effects of the structure and working parameters of the threshing device on the working performance of the threshing device (grain threshing rate, damage rate and impurity content) were studied, and the correlation between the working parameters of the threshing device and the working performance of the threshing device was obtained (Morishita and Suzuki, 2017; Xu et al., 2000; Tang et al., 2019; Chen et al., 2020). At the same time, some scholars have conducted bench tests on the threshing separation device composed of different types of threshing elements and different types of threshing rollers, which provides an important basis for the design and optimization of the threshing separation device, and obtains the optimized structural design scheme and operation parameter combination (Meusel et al., 2018; Su et al., 2020; Hosoi et al., 2020; Lenaerts et al., 2014).

In terms of cleaning, scholars mainly optimize the structural and working parameters of the cleaning device through performance tests, that is, for a certain type of cleaning device, study the influence laws of the physical and mechanical characteristic parameters of materials, the structural and motion parameters of the device and the air flow parameters formed by the fan on the cleaning performance and efficiency [12-14]. According to the distribution of the separated mixture, it is generally considered that the parts with a large amount of separated mixture require larger wind velocity airflow, and the parts with less mixture require a slightly lower wind velocity. In addition, the air flow generated by the fan needs to prevent the accumulation of separated mixture, and it is necessary to optimize the cleaning device to solve the poor cleaning effect caused by the accumulation of separated mixture (Chen et al., 2009; Chen et al., 2007).

The above-mentioned researches were conducted solely for the threshing or cleaning process, and most of designed test benches were also carried out in sections for threshing and cleaning. There were few studies on the comprehensive performance of the threshing-separating system under the interaction of the threshing drum and cleaning fan. Moreover, the existing studies are carried out under single-speed drum and cylindrical cleaning fan. It fails to fundamentally solve the problems of insufficient threshing capacity caused by the limited drum length of the horizontal axial-flow threshing-separating system and the influence of effluent accumulation at the inlet corner of the cleaning screen on the cleaning effect.

In order to solve the above problems, based on the researches of coaxial differential threshing and conical fan cleaning (Lachuga et al., 2020; Sahu and Raheman, 2020), a horizontal axial-flow threshing-separating device is designed in this paper. In order to explore the effects of working and structural parameters, such as differential drum speed combination, length ratio of high-low speed sections of differential drum, and the conical fan blade taper on the performance (loss rate, crushing rate, impurity content) and threshing power consumption of cross axial-flow separation device, the test-bed is designed based on the actual structure and size of the horizontal differential threshing-separating system. The performance test of the horizontal axial-flow threshing-separating device is carried out by using the quadratic rotation orthogonal combination design method. The influence degree of each factor on the performance index is analyzed, and the optimal combination of structural parameters and working parameters is obtained to provide a theoretical basis for optimizing the horizontal differential threshing-separating system.

MATERIALS AND METHODS

The horizontal axial-flow threshing-separating device is mainly composed of coaxial differential threshing-separating parts, air screen cleaning parts and spiral plate tooth residual re-thresher, as shown in Fig. 1. Its working principle is: (1) the tangentially fed materials are threshed by the axial-flow drum, and the effluents, mainly grains, are separated radially through the grid concave plate to the vibrating screen under the centrifugal force; (2) After falling down to the vibrating screen, the effluents are cleaned under the combination of the wind power of the conical centrifugal cleaning fan and double-layer vibrating screen; (3) Broken stems, leaves and glumes are blown out of the machine; (4) the clean grains are collected by the horizontal screw conveyor and sent to the grain collecting tank through the vertical screw conveyor; (5) Part of the residues falls on the tail of the vibrating screen and are collected by the residue horizontal screw conveyor, then sent to the re-thresher by the residue vertical screw conveyor and the materials after re-threshing return to the vibrating screen for secondary cleaning; (6) the threshed straws are discharged radially from the machine at one end of the high-speed drum.

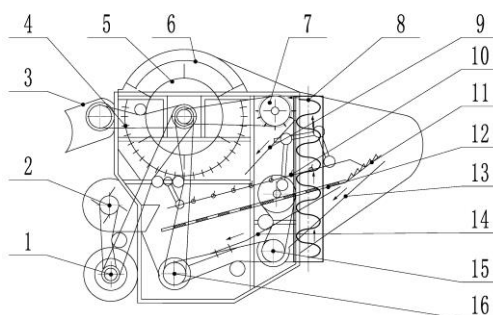


Fig.1 - Structure of differential axial-flow threshing-separating device

1. Transmission shaft; 2. Conical fan; 3. Conveyor; 4. Grid concave plate; 5. Rod tooth differential threshing drum; 6. Guide plate; 7. Re-thresher; 8. Residual vertical auger; 9. Stripper slide; 10. Upper sieve; 11. Tail sieve; 12. Lower sieve; 13. Residual recovery slide; 14. Grain collection slide; 15. Residual recycling auger; 16. Grain horizontal auger;

The coaxial differential threshing-separating part is composed of rod tooth differential threshing drum, grid concave sieve and cover with guide plate. The rod tooth differential threshing drum is shown in Fig. 2. The low speed section of the coaxial differential axial-flow drum is mainly used for the threshing-separating of most of easy-to-thrown grains. The high-speed drum is mainly used for the threshing-separating of a small amount of hard-to-thrown grains and the separation of unseparated seeds from the low-speed drum. Low-speed threshing is used to reduce the crushing of grains and stems, and high-speed threshing is used to reduce the net loss of threshing and improve the separating rate. The threshing-separating capacity of horizontal axial-flow threshing-separating system is improved without increasing the drum length.

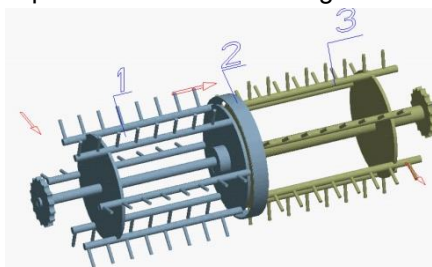


Fig. 2 - Three-dimensional model of rod tooth differential-speed threshing drum

1. Low-speed drum; 2. Anti-interference retaining ring; 3. High-speed drum;

The cleaning part is composed of conical centrifugal cleaning fan and double-layer vibrating screen. The structure of conical cleaning fan is shown in Fig. 3. The conical centrifugal cleaning fan uses the diameter difference between the large and small ends of fan blades to generate a wind pressure difference. It generates transverse wind in front of the vibrating screen to blow the falling leached material along the width of the screen, to avoid the leached material from accumulating at the corner of the vibrating screen surface entrance and improve the cleaning performance of the horizontal axial-flow threshing-separating system.

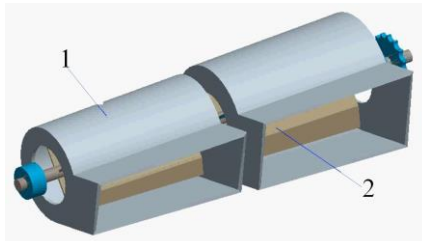


Fig. 3 - Three-dimensional model of conical centrifugal cleaning fan

1. Fan housing; 2. Fan blade

The horizontal differential threshing-separating system adopts innovative components, such as rod tooth differential threshing drum and conical centrifugal cleaning fan, to improve the threshing-separating comprehensive performance. However, the influence of working and structural parameters, such as the differential drum speed combination, the length ratio of high-low speed sections of the differential drum, and the conical fan blade taper, on the performance and threshing power consumption of the device is not clear. Thus, it needs to optimize the structure through experiments and master the influence degree of various factors on performance indicators.

Based on the actual structure and size of the horizontal differential threshing-separating system, the test bench developed is composed of a frame, a material conveying device, a feeding device, a threshing device, a cleaning device, and a measurement and control device, as shown in Fig.4.

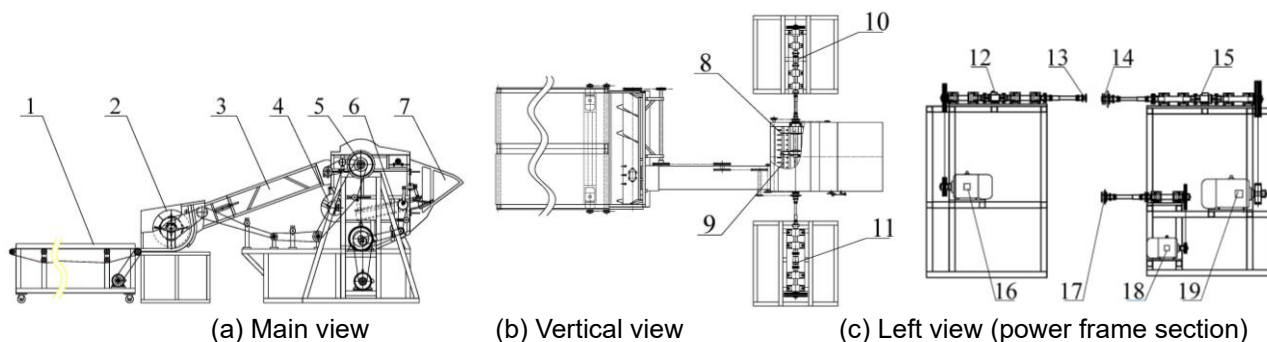


Fig.4 - Schematic diagram of the test bench

1. Material conveyor; 2. Feed auger; 3. Conveyor components; 4. Conical cleaning fan; 5. Differential threshing drum; 6. Double layer vibrating screen; 7. Impurity outlet; 8. High-speed drum; 9. Low-speed drum; 10. Power input shaft of high-speed drum; 11. Power input shaft of low-speed drum; 12. Torque sensor of high-speed drum; 13. Universal coupling of high-speed drum; 14. Universal coupling of low-speed drum; 15. Torque sensor of low-speed drum; 16. Drive motor of high-speed drum; 17. Universal coupling of cleaning fan; 18. Drive motor of cleaning fan; 19. Drum motor of low-speed drum

There are 4 sets of material conveying devices in total, and each size is: 5000(length) × 900(Width) mm with adjustable height and can be used in series or parallel. The speed of parallel conveying belt can be adjusted according to the requirements of different feeding, and the conveying speed is 0-2 m/s. The tension of the parallel conveyor belt can be adjusted by adjusting the position of the tension wheel.

The power of low-speed drum drive motor is 20 kW and the speed is 500-1000 r/min, and that of high-speed drum drive motor is 10 kW and the speed is 600-1200 R/min. A Beijing WorldCom T-660 torque sensor is equipped at both ends of the high and low speed threshing drums, with measuring ranges of 0 ± 100 Nm and 0 ± 300 Nm respectively to measure the torque, speed and power of high and low-speed drums. According to the test scheme, there are 5 sets of differential threshing rollers. The diameter of each set of high and low speed drums is 550 mm; the wrap angle of the grid concave plate is 230° ; the helix angle of the cover guide plate is 32° , and the total working length of the threshing drum (including the high and low speed sections) is 1000 mm, which shall be replaced as a whole. According to the requirements of the test scheme, 5 sets of fan blades with different tapers are configured, and the fan blades are replaced as required during the test.

The measurement and control device is mainly composed of electrical control system and data acquisition system. The power supply of the electrical control system is a standard three-phase four-wire system, three-phase AC power 380 V and 50 HZ. The electrical control cabinet is equipped with frequency converter, control transformer, automatic air switch, AC contactor, bridge rectifier, small intermediate relay, multi-functional socket, and wiring block. The door of the control cabinet is equipped with main start button, emergency stop button, inverter digital operator (including inverter parameter setting and adjustment of attached potentiometer, ON/OFF switch) and indicator lights. The data acquisition system consists of a torque sensor, a data acquisition card, a USB connection and a computer. The speed, torque and power at both ends of the high and low speed drums are automatically saved on the computer and displayed graphically in real time.

Before the test, the crop conveying speed is set according to the feeding amount; the time from the start of the conveying table to the set speed is measured, and the reserved space at the front end of the conveying table without crops is calculated. According to the set feeding amount (2 kg/s), in each group of experiments, rice of equal quality is evenly spread within the specified range of the conveyor belt. The length of stalks is consistent with the conveying direction, and the ears are facing forward to ensure feed evenly and quantitatively. According to the test plan, five differential drums with different length ratios and five fan blades with different tapers are installed. The speed of high-low speed drums and conveyor table are adjusted through the frequency converter.

During the test, start the motor switches of high-speed drums, low-speed drums and cleaning device in sequence. After the preset working parameters of the rotating parts are reached and stabilized, start the measurement and control system software, and finally turn on the motor switch of the material conveyor.

The test was carried out indoors. The experimental rice used "Yongyou No. 15" widely planted in Zhejiang Province, and the test was carried out on the same day after manual harvesting (cutting height 150 mm). Some characteristics of rice are shown in Table 1.

Table 1

Basic properties of the test rice	
Item	Parameters
Material plant height /cm	100-115
Ear length/cm	17.5-26.4
Grain moisture content /%	23.3-24.5
Stem moisture content /%	45.4-48.6
Grass Valley ratio(Stubble cutting 15cm)	3:1
1000 grain weight of rice /g	30.6
Unit yield / kg/hm ²	10020

On the self-developed test bench, the horizontal axial-flow threshing-separating device was tested for rice threshing-separating. Investigate the three main factors: differential drum speed combination (speed combination x_1), the length ratio of high and low speed sections of the differential drum (high-speed section ratio x_2), and the conical fan blade taper (blade taper x_3) on the performance of threshing and cleaning device (Loss rate y_1 , crushing rate y_2 , impurity rate y_3 , threshing power consumption y_4). The test is repeated twice, and the site is shown in Fig. 5.



Fig. 5 – Experimental site

The test plan is designed by the quadratic orthogonal rotation combination design method, and the value range of each test factor is determined according to the theoretical analysis and actual production. A more ideal factor level is initially selected, and the factor level coding is shown in Table 2.

Table 2

Coding value x_j	Coding of factor level		
	Speed combination x_1 (r/min)	High-speed section ratio x_2 (%)	Blade taper x_3 (°)
Upper asterisk arm (+ γ)	918/1018	46.8	3.8
Upper level (+1)	850/950	40	3.5
Zero level (0)	750/850	30	3
Lower level (-1)	650/750	20	2.5
Lower asterisk arm (- γ)	582/682	13.2	2.2

After the test, collect and clean up the discharge from the grass and the cleaning room outlet, and calculate the loss rate (including uncleaned kernels, entrainment loss and cleaning loss), and take samples from the grain outlet to determine the crushing rate and impurity content. The material collection area in the test is shown in Fig. 6.



Fig. 6 - Material collecting area after experiment

RESULTS

According to the feeding amount and the grass to grain ratio, the total grain mass obtained in each experiment was obtained, and recorded as W . A sample from the receiving grain was taken and the total mass was recorded as W_1 . The broken grains and impurities were manually selected and weighed separately, and recorded as $W_{broken\ 1}$ and $W_{impurities\ 1}$, respectively. All the effluents were collected from the cleaning room and the grass discharge outlet. The grains and the ears with grains were selected manually, and weighed, and then they were recorded as the cleaning loss $W_{cleaning}$ and the entrainment loss $W_{entrainment}$, respectively.

The loss rate y_1 , crushing rate y_2 and impurity rate y_3 are obtained through the following formulas:

$$y_1 = \frac{(W_{cleaning} + W_{entrainment})}{W} \tag{1}$$

$$y_2 = \frac{W_{crushing1}}{W_1} \tag{2}$$

$$y_3 = \frac{W_{impurity1}}{W_1} \tag{3}$$

According to the ternary quadratic orthogonal rotation combination design, the experiment was arranged and 23 experiments were carried out. The experiment scheme and results are shown in Table 3.

Table 3

Experiment program and results for quadratic regression orthogonal rotation

No.	Speed combination x_1 (r/min)	High-speed section ratio x_2 (%)	Blade taper x_3 (°)	Loss rate y_1 (%)	Crushing rate y_2 (%)	Impurity rate y_3 (%)	High-speed drum power consumption (kW)	Low-speed drum power consumption (kW)	Total power consumption of threshing (kW)
1	850/950	40	3.5	2.69	0.82	0.64	5.96	10.79	16.75
2	850/950	40	2.5	1.95	0.86	0.85	6.17	10.32	16.49
3	850/950	20	3.5	1.98	0.77	0.78	5.32	10.19	15.51
4	850/950	20	2.5	2.33	0.84	0.98	5.22	10.23	15.45
5	650/750	40	3.5	1.78	0.49	0.32	4.78	9.16	13.94
6	650/750	40	2.5	1.56	0.51	0.49	4.86	8.39	13.25
7	650/750	20	3.5	1.44	0.44	0.31	4.55	8.12	12.67
8	650/750	20	2.5	1.68	0.34	0.96	4.58	7.44	12.02
9	582/682	30	3	0.88	0.35	0.39	4.14	7.17	11.31
10	918/1018	30	3	2.78	0.98	0.78	6.12	13.7	19.82
11	750/850	13.2	3	1.35	0.78	0.79	5.02	9.12	14.14
12	750/850	46.8	3	1.45	0.57	0.88	4.99	11.23	16.22
13	750/850	30	2.2	1.38	0.41	0.78	5.11	8.40	13.51
14	750/850	30	3.8	1.57	0.71	0.38	5.43	7.90	13.33
15	750/850	30	3	1.43	0.54	0.47	5.78	8.23	14.01
16	750/850	30	3	1.24	0.58	0.43	5.55	9.24	14.79
17	750/850	30	3	1.33	0.64	0.53	4.98	9.17	14.15
18	750/850	30	3	1.21	0.44	0.47	5.23	9.68	14.91
19	750/850	30	3	1.48	0.53	0.48	5.41	9.22	14.63
20	750/850	30	3	1.11	0.58	0.39	4.76	9.27	14.03
21	750/850	30	3	1.09	0.61	0.51	4.78	9.7	14.48
22	750/850	30	3	1.47	0.57	0.45	5.13	9.89	15.02
23	750/850	30	3	1.23	0.49	0.48	5.23	9.38	14.61

According to the results of 23 experiments, using the "experimental statistics"-quadratic orthogonal rotation combination design" in the DPS data processing system, the ternary quadratic regression equation of the loss rate can be obtained as:

$$y_1 = 1.28 + 0.42x_1 + 0.05x_2 + 0.05x_3 + 0.26x_1^2 + 0.11x_2^2 + 0.14x_3^2 + 0.11x_1x_2 + 0.05x_1x_3 + 0.19x_2x_3 \tag{4}$$

where, y_1 - loss rate, %; y_2 - crushing rate, %; y_3 - impurity rate, %; y_4 - threshing power consumption, kW; x_1 - speed combination, r/min; x_2 - high-speed drum ratio, and x_3 - blade taper, °.

The results of the variance analysis of the regression equation are shown in Table 4.

Table 4

Results of variance analysis of loss rate regression equation

Source	Sum of square	Freedom	F ratio
Regression	4.33	9	$F_2=7.68$
Surplus	0.81	13	
Lack-of-fit	0.33	5	
Error	0.17	8	$F_1=1.94$
Total	5.14	22	

$F_1=1.94 < F_{0.05}(5,8) = 3.69$ shows the lack of fit is not obvious. This indicates that, in the sum-lack-of-fit squares, other non-negligible factors have little impact on the test results. The statistical quantity F_2 can be used to test the significance of regression equation. $F_2=7.68 > F_{0.01}(9,13) = 4.17$, the result of F test shows that the regression equation obtained by the regression orthogonal rotation design fits the actual situation well, and the equation has practical significance. After t-test, the insignificant items are eliminated, and the regression equation can be obtained as:

$$y_1 = 1.28 + 0.42x_1 + 0.26x_1^2 + 0.11x_2^2 + 0.14x_3^2 + 0.19x_2x_3 \tag{5}$$

Using the same method, the regression equations of crushing rate, loss rate and threshing power consumption are respectively:

$$y_2 = 0.55 + 0.19x_1 + 0.03x_3 + 0.04x_1^2 + 0.04x_2^2 - 0.02x_1x_2 - 0.03x_1x_3 \tag{6}$$

$$y_3 = 0.47 + 0.13x_1 - 0.04x_2 - 0.14x_3 + 0.04x_1^2 + 0.13x_2^2 + 0.06x_2x_3 \tag{7}$$

$$y_4 = 14.52 + 1.95x_1 + 0.61x_2 + 0.33x_1^2 - 0.43x_3^2 - 0.13x_1x_3 \tag{8}$$

There are three variables in the regression equation. In order to find out the influence of each factor on each index intuitively, the dimensionality reduction method is used to transform the multivariate complex problem into a one-dimensional problem, i.e., two of the three factors are taken to a fixed level, and the influence of the remaining factors on each index is observed. For example, when investigating the influence of speed combination, high-speed section ratio, and blade taper on the loss rate, let the regression equation (5) $x_2=x_3=0$; $x_1=x_3=0$; $x_1=x_2=0$ respectively, the following equations are obtained:

$$y_1 = 1.28 + 0.42x_1 + 0.26x_1^2 \tag{9}$$

$$y_1 = 1.28 + 0.11x_2^2 \tag{10}$$

$$y_1 = 1.28 + 0.14x_3^2 \tag{11}$$

Equations (9)-(11) respectively represent the relationship between speed combination, high-speed drum ratio, blade taper and loss rate, and draw the influence curve of each factor on the loss rate, as shown in Fig. 7.

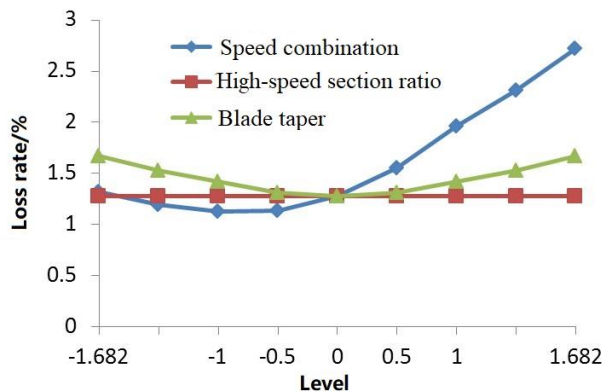


Fig. 7 - Impact of each factor on loss rate

From Fig. 7, when the drum speed is low, the loss is greater, because the threshing is incomplete, and the non-threshing loss is large. When the drum speed is greater than -1, the loss rate becomes larger as the rotational speed increases. When the drum speed exceeds 1, the trend is more obvious. This is because that, when the speed of threshing drum exceeds a certain range, the loss of grain crushing increases. When the speed-length ratio of the drum is constant, the loss first decreases and then increases with the fan blade taper. At 0 level, the loss rate is the smallest, indicating that the transverse wind energy produced by the conical fan effectively reduces the loss rate. However, with the increase of the fan blade taper, the distribution of cleaning screen becomes worse due to excessive transverse air. Some grains are blown out of the machine, resulting in greater cleaning loss. The order of the factors affecting the loss rate is: speed combination, blade taper and high-speed drum ratio.

According to the above method, the single factor influence curves of speed combination, high-speed drum ratio and blade taper with crushing rate, impurity content and threshing power consumption can be obtained, as shown in Fig. 8, Fig. 9, Fig. 10.

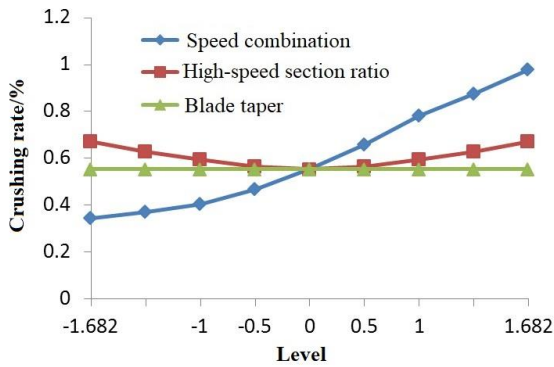


Fig. 8 - Impact of each factor on crushing rate

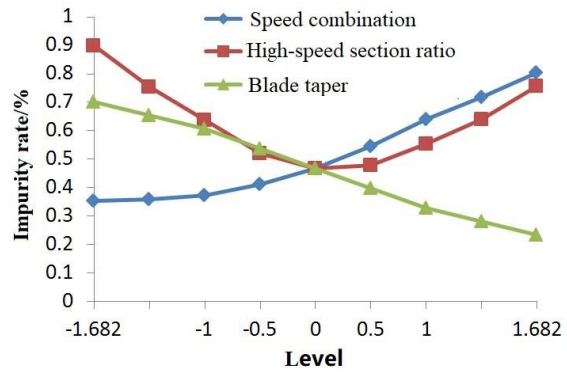


Fig. 9 - Influence of each factor on impurity rate

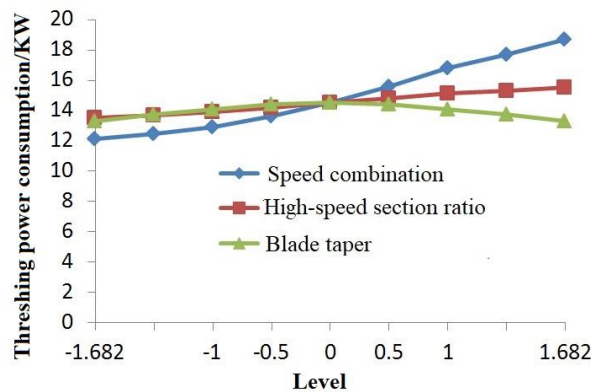


Fig. 10 - Influence of each factor on threshing power consumption

From Fig.8, the combination of drum speed and crushing rate is obviously positively correlated, i.e., the higher the drum speed, the greater the crushing rate. When the high-speed drum section ratio is small, the crushing rate is larger. This is because the low drum speed affects the separation of seeds. As the high-speed section ratio increases, the crushing rate becomes smaller, and the crushing rate is the smallest at 0. Subsequently, as the high-speed section ratio increases, the crushing rate increases. This indicates that the length ratio of high-low speed drums has a significant impact on the crushing rate, and the high speed section ratio should not be too small or too large, and 0 is more appropriate. The influence curve of fan blade taper on the crushing rate tends to a straight line, indicating that the fan blade taper has little effect on the crushing rate. The order of the factors that affect the crushing rate is speed combination, high-speed section ratio and blade taper.

From Fig. 9, the higher the drum speed, the higher the impurity content. The trend of speed combination above 0 level is more obvious, indicating that with the increase of the drum speed, the broken stems and leaves in the threshing space increase. This increases the impurity content of grains. The high-speed section has a small proportion and a large impurity rate. As the high-speed section ratio increases, the impurity rate becomes smaller, and the impurity rate is the smallest at 0 level. Subsequently, as the high-speed section ratio increases, the impurity rate increases, indicating that the high-speed section ratio should not be too small or too large, and 0 is more appropriate. The influence of fan blade taper on impurity content is significant. With the increase of blade taper, the impurity content decreases, indicating that the transverse air of conical cleaning fan plays an important role in cleaning quality. The order of the factors affecting the impurity content is speed combination, blade taper and high-speed section ratio.

From Fig. 10, the threshing power consumption increases with the increase of the drum speed and the high-speed section ratio. However, the drum speed has a greater impact on the threshing power consumption than the two, and the fan blade taper has little effect on threshing power consumption. When the blade taper is 0, it is slightly greater than other levels. The order of the factors affecting threshing power consumption is speed combination, high-speed section ratio and blade taper.

In the ternary quadratic regression equation, fix one of the factors to get the regression sub-model of the other two factors and indicators. In formula (5), let $x_3=0$, $x_2=0$ and $x_1=0$, then the two factor equations of loss rate are:

$$y_1(x_1, x_2) = 1.28 + 0.42x_1 + 0.26x_1^2 + 0.11x_2^2 \tag{12}$$

$$y_1(x_1, x_3) = 1.28 + 0.42x_1 + 0.26x_1^2 + 0.14x_3^2 \tag{13}$$

$$y_1(x_2, x_3) = 1.28 + 0.11x_2^2 + 0.14x_3^2 + 0.19x_2x_3 \tag{14}$$

The surface diagram method is used to describe the influence of two factors on the test index. The two-factor influence surface diagram of the test index is drawn in Matlab, as shown in Fig. 11. Fig. 11(a) is the two-factor influence surface diagram of the speed combination and high-speed section ratio on the loss rate. Fig. 11(b) is a curved surface diagram of the two-factor influence of the speed combination and the blade taper on the loss rate. Fig. 11(c) is a curved surface diagram of the two-factor effect of the high-speed section ratio and blade taper on the loss rate.

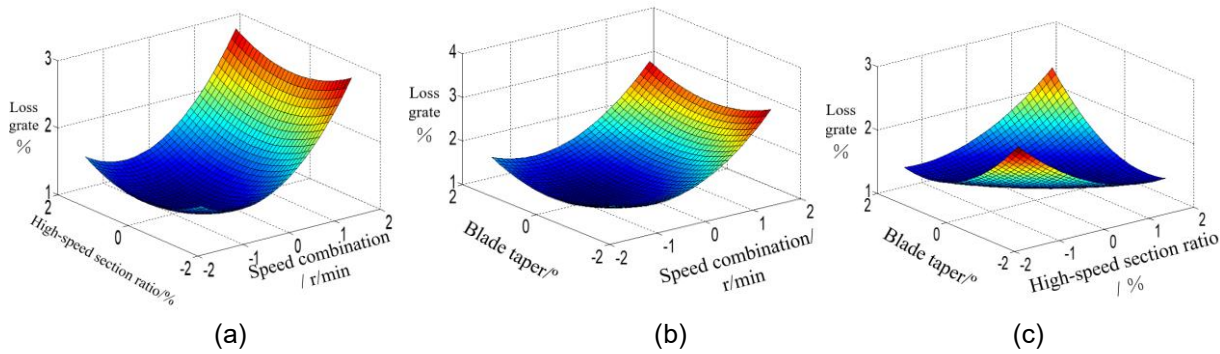


Fig. 11 - Impact of two factors on loss rate

From Fig. 11(a), in the interaction of the drum speed combination and high-speed section ratio, the speed combination has a greater impact on the loss rate. When the speed combination is -1 level and the high-speed section ratio is 0 level, the loss rate is the smallest. From Fig. 11 (b), in the interaction between the combination of drum speed and fan blade taper, the speed combination has a greater impact on the loss rate. When the speed combination is -1 level and the fan blade taper is 0 level, the loss rate is the smallest. From Fig. 11 (c), in the interaction between the high-speed section ratio and fan blade taper, when they are both at 0 level, the loss rate is the smallest.

Using the same method above, the two factor influence surface diagram of crushing rate, impurity content and total threshing power consumption can be obtained, as shown in Fig. 12, Fig. 13 and Fig. 14.

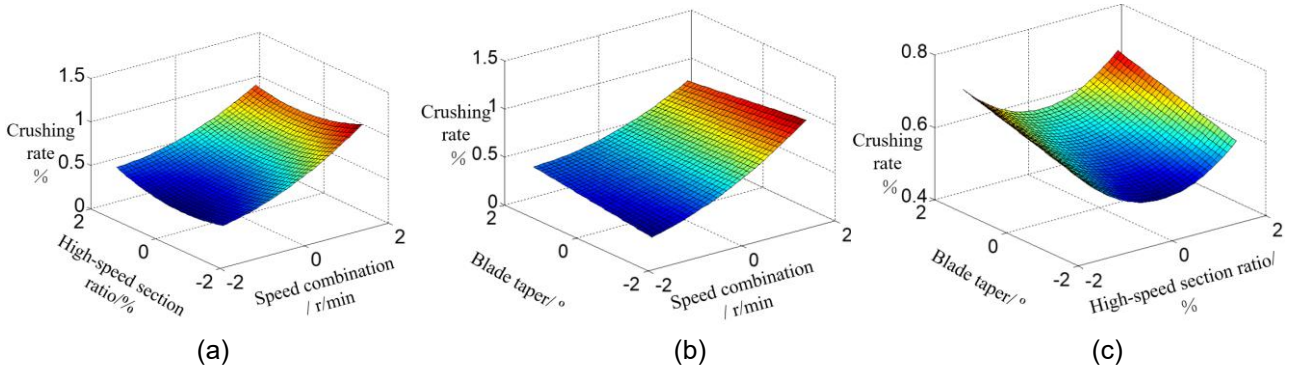


Fig. 12 - Two factor influence surface diagram of crushing rate

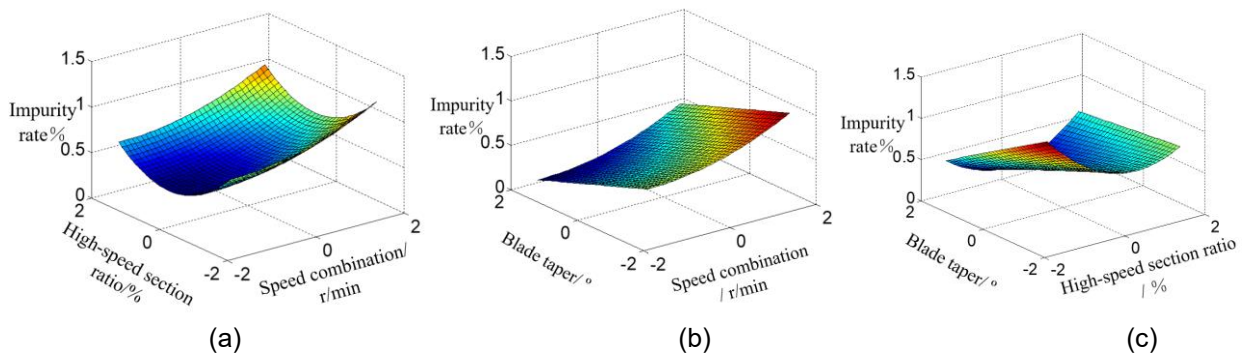


Fig.13 - Two factor influence surface diagram of impurity rate

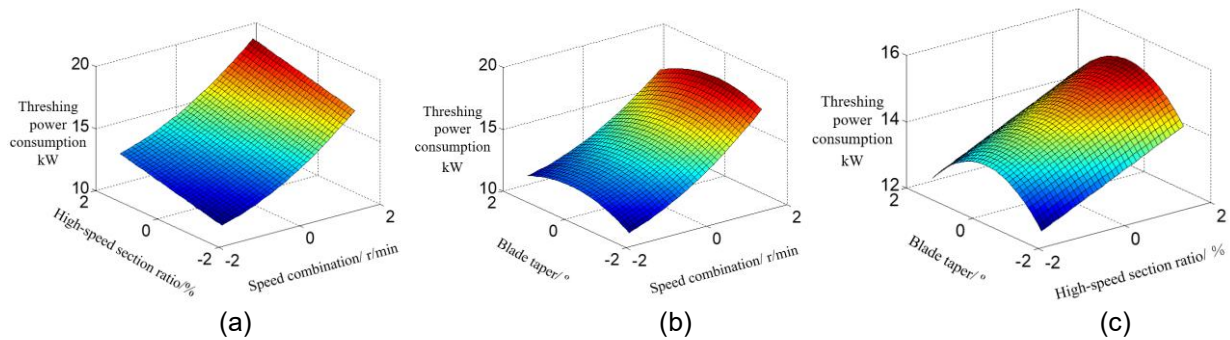


Fig.14 - Two factor influence surface diagram of threshing power consumption

From Fig. 12 (a), in the interaction between the drum speed combination and the drum high-speed section ratio, when the high-speed section ratio is 0 level, the crushing rate increases with the increase of speed. From Fig. 12 (b), the drum speed combination has a great impact on the crushing rate. When the speed is low, the crushing rate increases slightly with the increase of the blade taper; while when the speed is high, the crushing rate decreases slightly with the increase of the blade taper. From Fig. 12 (c), when the high-speed section ratio is 0 and the fan blade taper is -1.682, the crushing rate is the smallest, and the crushing rate increases with the increase of the fan blade taper.

According to Fig. 13 (a), in the interaction between the drum speed combination and the drum high-speed section ratio, when the proportion of the high-speed section is 0, the impurity content increases with the increase of the speed. When the high-speed section ratio and speed combination are at the maximum level, the impurity content is the largest. From Fig. 13 (b), the crushing rate increases with the increase of speed and decreases with the increase of fan blade taper. From Fig. 13 (c), when the fan blade taper and the high-speed section ratio are at the minimum level, the impurity content is the maximum. When the high-speed section ratio is at 0 level and the blade taper is at the maximum level, the impurity content is the minimum.

From Fig. 14(a), in the interaction of the speed combination and high-speed section ratio of the drum, the threshing power consumption is obviously positively correlated with the speed combination and the high-speed section ratio. From Fig. 14(b), in the interaction between drum speed combination and fan blade taper, speed combination is the main factor. From Fig. 14 (c), the threshing power consumption increases with the increase of the high-speed section ratio when the fan blade taper is 0 level.

Loss rate, crushing rate, impurity content and threshing power consumption are the main indexes to evaluate the performance of the threshing-separating device, which should reach the minimum value under their respective constraints. According to the established mathematical models of loss rate y_1 , crushing rate y_2 , impurity rate y_3 , and threshing power consumption y_4 , let:

$$y_i = f(x_1, x_2, x_3) \rightarrow \min \quad (i = 1,2,3,4) \quad (15)$$

Multi-objective optimization method is used to analyze the best parameter combination of the comprehensive performance of threshing-separating, and the optimization toolbox *fgoalattain* function in MATLAB is used to solve the multi-objective achievement problem. The constraint conditions are:

$$\begin{cases} y_i \geq 0 \\ -1.682 \leq x_j \leq 1.682 \quad (i = 1,2,3,4; j = 1,2,3) \end{cases}$$

The optimal combination parameter scheme of the horizontal axial-flow threshing-separating device is as follows: the level value of speed combination x_1 is 0.0307, and the actual value is 773/876 r/min; the level value of high-speed section ratio x_2 is -0.0167, and the actual value is 29.5%; the level value of fan blade tape x_3 is 1.6791 and the actual value is 3.75°. According to the level change range of each factor in the experimental design, the three-factor optimal parameter combination scheme is finally selected as: 750/850 r/min of the speed combination, 30% of the high-speed section ratio and 3.8° of the blade taper. It can be seen that the 14th set of the 23 experimental programs is the best. Under this condition, the horizontal axial-flow threshing-separating device is optimal, with 1.57% of loss rate, 0.71% of crushing rate, 0.38% of impurity rate, and 13.33 kW of total threshing power consumption. The average power consumption of low-speed drum accounts for 59.3% of the total threshing-separating power consumption, and that of high-speed drum accounts for 40.7%.

In order to verify the performance of the horizontal axial-flow threshing-separating device, in October 2015, under the auspices of a third-party professional testing organization, a field test was carried out in Zhiying Town, Yongkang City, Zhejiang Province, as shown in Fig. 15. The test was carried out on a full-feed combine harvester equipped with a horizontal axial-flow threshing-separating device. The structural parameters and working parameters take the best combination of parameters obtained by multi-objective optimization. The tested rice varieties and feed rates were consistent with the bench test, and they were "Yongyou 15" and 2 kg/s, respectively. The field test results are shown in Table 5. The results show that the loss rate, impurity content rate and crushing rate of the horizontal axis-flow threshing-separating device are better than the national standards.



Fig. 15 - Field trial

Table 5

Results of field trials			
Test items	Total loss rate /%	Impurity rate /%	Crushing rate /%
Standard requirements test results	≤3.0	≤2.0	≤1.0
	1.78	0.44	0.65

CONCLUSIONS

(1) The horizontal axial-flow threshing-separating device test bench can carry out multi-scheme coaxial differential threshing and separating, and air-screen cleaning performance tests. The coaxial differential threshing technology solves the contradiction between the loss rate (dirty removal and entrainment) and crushing rate by rationally using the threshing drum speed. The transverse wind generated by the conical cleaning fan can effectively evenly distribute the leached material on the vibrating screen.

(2) The order of the three factors that affect the loss rate and impurity rate of the horizontal axial-flow threshing-separating device is the combination of differential drum speed, conical fan blade taper, and the length ratio of high and low speed sections of the differential drum. The order of the three factors affecting the crushing rate and threshing power consumption of the horizontal axial-flow threshing-separating device is the differential drum speed combination, the length ratio of high and low speed sections of the differential drum, and the conical fan blade taper.

(3) The optimal parameter combination is: 750/950 r/min of the differential drum speed, 3.8° of fan blade taper, and 30% of high-speed section ratio. The corresponding work performance indicators are 1.57% of loss rate, 0.71% of crushing rate, 0.38% of impurity rate and 6.67 kW/kg of threshing power consumption.

ACKNOWLEDGEMENT

The work was supported by the National Natural Science Foundation of China (51305182) and Public welfare research project of science and Technology Department of Zhejiang Province (2017C32097).

REFERENCES

- [1] Chen, D. J., Gong, Y. J., Huang, D. M. Xiong, Y. S., Chen, N., Wang, Y. Z. (2007). Development on some apparatus of Chinese model caterpillar rice-wheat combine harvester (履带式全喂入稻麦联合收获机工作装置设计), *Transactions of the Chinese society for agricultural machinery*, Vol. 38(8), 82-85, Beijing/China.

- [2] Chen, J., Lian, Y., Li, Y. M. (2020). Real-time grain impurity sensing for rice combine harvesters using image processing and decision-tree algorithm, *Computers and electronics in agriculture*, Vol. 175, 105591. England.
- [3] Chen, N., Huang, D. M., Chen, D. J., Tian, X. J., Zhang, J. R. (2009). Theory and experiment on non-uniform air-flow cleaning of air-screen cleaning unit (风筛式清选装置非均布气流清选原理与试验), *Transactions of the Chinese Society for Agricultural Machinery*, Vol. 40(4), 73-77, Beijing/China.
- [4] Chen, N., Xiong, Y. S., Chen, D. J., Xu, J. D., Zhao, Y. (2010). Design and test on the coaxial differential-speed axial-flow threshing rotor of combine harvester (联合收获机同轴差速轴流脱粒滚筒设计和试验), *Transactions of the Chinese Society for Agricultural Machinery*, Vol. 41(10):67-71, Beijing/China.
- [5] Hosoi, J., Ushiki, J., Sakai, N., Aoki, M., Tezuka, M. (2008). Seed shattering habit of weedy rice (*Oryza saliva*) in Nagano prefecture, Japan, and germination ability of shattered seeds, *Japanese Journal of Crop Science*, Vol. 77(3), 321-325, Japan.
- [6] Lachuga, Y. F., Bur'Yanov, A. I., Pakhomov, V. I. (2020). Chervyakov I.V., Adaptation of Threshing Devices to Physical and Mechanical Characteristics of Harvested Crops, *Russian Agricultural Sciences*, Vol. 46, 198-201, Russia.
- [7] Lenaerts, B., Aertsen, T., Tijsskens, E., De, K. B., Ramon, H. (2014). De Baerdemaeker J., Saeys W., Simulation of grain-straw separation by Discrete Element Modeling with bendable straw particles, *Computers and Electronics in Agriculture*, Vol. 101: 24-33. England.
- [8] Li, Y. M., Su, Z., Liang, Z. W., Li, Y. (2020). Variable-Diameter Drum with Concentric Threshing Gap and Performance Comparison Experiment, *Applied sciences*, Vol. 10(15):5386. Romania
- [9] Li, Y. M., Wang, C. H., Xu, L. Z., Li, L., Xue, Z. (2014). Parameter optimization and field test of threshing and separation device in tangential-longitudinal combine (切纵流联合收获机脱粒分离装置田间试验与参数优化), *Transactions of the Chinese Society for Agricultural Machinery*, Vol. 45(11), 111-116, Beijing/China.
- [10] Liu, Z. H., Dai, S. J., Li, M. Q., Chen, N., Wang, Z. P., Chen, D. J. (2018). Design and test of the head-feeding harvester's moving grate concave unit (半喂入联合收割机活动栅格凹板装置设计与试验), *Journal of Chinese Agricultural Mechanization*, Vol. 39(5), 9-14, Jiangsu/China.
- [11] Meusel, C., Kieu, D., Gilbert, S., Luecke, G., Gilmore, B., Kelly, N., Hunt, T. (2018). Evaluating operator harvest technology within a high-fidelity combine simulator, *Computers and Electronics in Agriculture*, Vol. 148, 309-321, England.
- [12] Miu, P. I., Kutzbach, H.-D. (2007). Mathematical model of material kinematics in an axial threshing unit, *Computers and Electronics in Agriculture*, Vol. 58(2), 93-99, England.
- [13] Miu P. I., Kutzbach, H.-D. (2008). Modeling and simulation of grain threshing and separation in threshing units-Part I, *Computers and Electronics in Agriculture*, Vol. 60(1), 96-104, England.
- [14] Morishita, T., Suzuki, T. (2017). The evaluation of harvest loss occurring in the ripening period using a combine harvester in a shattering-resistant line of common buckwheat, *Japanese Journal of Crop Science*, Vol. 86(1), 62-69, Japan.
- [15] Sahu, G., Raheman, H. (2020). Development of a Renewable Energy Operated Paddy Thresher. *Journal of the Institution of Engineers (India): Series A*, Vol.101 (4), 657-668, India.
- [16] Su, Z., Li, Y. M., Dong, Y. H., Tang, Z., Liang, Z. W. (2020). Simulation of rice threshing performance with concentric and non-concentric threshing gaps, *Biosystems Engineering*, Vol. 197, 270-284, England.
- [17] Tang, Z., Li, Y., Li, X.Y., Xu, T. B. (2019). Structural damage modes for rice stalks undergoing threshing, *Biosystems Engineering*, Vol. 186, 323-336, England.